WILEY

Author Query Form

Journal MICE

Article mice12813

Dear Author,

During the copyediting of your manuscript the following queries arose.

Please refer to the query reference callout numbers in the page proofs and respond.

Please remember illegible or unclear comments and corrections may delay publication.

Many thanks for your assistance.

Query No.	Description	Remarks
Q1	Please confirm that forenames/given names (blue) and surnames/family names (vermilion) have been identified correctly.	
Q2	Please check the affiliation for correctness.	
Q3	The term "PDW" has been defined as the "performance degree of WDN" to maintain consistency in this article. Please check for correctness.	
Q4	The reference "Rossman, 2020" has been updated as "Rossman et al. 2020" to match the references list. Please check for correctness.	
Q5	Please check whether the edits in the sentence beginning "In this study, the system state is..." retain the intended sense.	
Q6	The reference "Sutton & Barto, 2018" is cited in the text but is not listed in the references list. Please either delete the in-text citation or provide full reference details following journal style.	
Q7	Please check Table 2 caption for correctness.	
Q8	Please check whether the edits in the sentence beginning "The PDW considers the NSDs, which measure..." retain the intended sense.	
Q9	Please provide the URL for reference "Alliance, 2001".	
Q10	Please update reference "Kipf and Welling, 2016", if already published.	
Q11	Please update reference "Li et al., 2017", if already published.	
Q12	Please update reference "Mnih et al., 2013", if already published.	
Q13	Please update reference "Wang et al., 2019", if already published.	
Q14	Please check reference "Wiering and Van Otterlo, 2012" for correctness.	

DOI: 10.1111/mice.12813

ORIGINAL ARTICLE

COMPUTER-AIDED CIVIL AND INFRASTRUCTURE ENGINEERING WILEY

A graph convolution network-deep reinforcement learning model for resilient water distribution network repair decisions

Xudong Fan | Xijin Zhang | Xiong (Bill) Yu

Department of Civil and Environmental Engineering, Case Western Reserve University, Cleveland, Ohio, USA

Correspondence
Xiong (Bill) Yu, Department of Civil and Environmental Engineering, Case Western Reserve University, 2104 Adelbert Road, Bingham 206, Cleveland, OH 44106-7201, USA.
Email: xxy21@case.edu

Funding information
US National Science Foundation, Award No. 1638320
European Research Council, Grant/Award Number: 64659
https://doi.org/10.1111/mice.12577
US National Science

Abstract

Water distribution networks (WDNs) are critical infrastructure for communities. The dramatic expansion of the WDNs associated with urbanization makes them more vulnerable to high-consequence hazards such as earthquakes, which requires strategies to ensure their resilience. The resilience of a WDN is related to its ability to recover its service after disastrous events. Sound decisions on the repair sequence play a crucial role to ensure a resilient WDN recovery. This paper introduces the development of a graph convolutional neural network-integrated deep reinforcement learning (GCN-DRL) model to support optimal repair decisions to improve WDN resilience after earthquakes. A WDN resilience evaluation framework is first developed, which integrates the dynamic evolution of WDN performance indicators during the post-earthquake recovery process. The WDN performance indicator considers the relative importance of the service nodes and the extent of post-earthquake water needs that are satisfied. In this GCN-DRL model framework, the GCN encodes the information of the WDN. The topology and performance of service nodes (i.e., the degree of water that needs satisfaction) are inputs to the GCN; the outputs of GCN are the reward values (Q-values) corresponding to each repair action, which are fed into the DRL process to select the optimal repair sequence from a large action space to achieve highest system resilience. The GCN-DRL model is demonstrated on a testbed WDN subjected to three earthquake damage scenarios. The performance of the repair decisions by the GCN-DRL model is compared with those by four conventional decision methods. The results show that the recovery sequence by the GCN-DRL model achieved the highest system resilience index values and the fastest recovery of system performance. Besides, by using transfer learning based on a pre-trained model, the GCN-DRL model achieved high computational efficiency in determining the optimal repair sequences under new damage scenarios. This novel GCN-DRL model features robustness and universality to support optimal repair decisions to ensure resilient WDN recovery from earthquake damages.

1 | INTRODUCTION

Multiple hazards that occurred in recent years have drawn increasing attention to ensuring the resilience of community infrastructures. Critical infrastructure networks, including the water distribution networks (WDNs), gas supply networks, transportation networks, and power grid networks, are the cornerstones for resilient community services (Karakoc et al., 2019). As critical infrastructure, WDNs play important roles in ensuring the quality of life and community functions. Buried pipelines have experienced a large number of damages during past earthquakes (Nair et al., 2018; Pudasaini & Shahandashti, 2018). For example, 3039 pipe failures were identified after the Christchurch earthquake on February 22, 2011 (Eidinger & Tang, 2014). The "effective" completion of the total repairing work, which returned the WDNs service to the minimal level of satisfaction, took about 53 days (T. D. O'Rourke et al., 2014). Disruption of WDNs after earthquakes not only caused huge economic loss but also raised serious public health concerns. Efficient post-earthquake recovery of WDN improves the resilience of WDNs, which requires analyzing its seismic resilience and developing novel methods for resilience improvements.

The term "resilience" is originally derived from the Latin word "resilo" with the meaning "bounce back" (Hosseini et al., 2016), which describes the ability of a system or material or physical structure to bear a disruption and return to its original performance. For a water distribution system, resilience can be described as its ability to resist disruptive hazards (such as natural or man-made hazards) and quickly restore its service after such disruptions. Correspondingly, the methods for resilience quantification can be broadly divided into two major categories, that is, surrogate-based resilience quantification method and performance-based resilience quantification method. The surrogate-based quantification method treats the WDNs as static systems (typically before disruption) without considering their time-dependent performance during or after the disruption (Jayaram & Srinivasan, 2008; Prasad et al., 2004; Pudasaini & Shahandashti, 2020; Todini, 2000; Zarghami et al., 2018). However, when it comes to the WDN post-hazard management, the performance-based method can provide a more straightforward evaluation method and therefore has been widely used. Previous studies have proposed different system performance metrics and attack–recovery strategies to evaluate infrastructure resilience, (Diao et al., 2016; Sharkey et al., 2021) gave a detailed review of the related metrics. The commonly considered factors for the system performance evaluation include the water availability, water quality, and

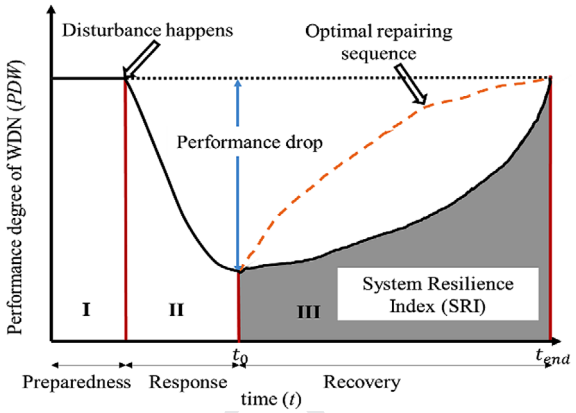

FIGURE 1 Illustration of the water distribution network (WDN) system performance prior, during, and after disruption by hazards, the characteristics of which define system resilience (t_0 and t_{end} denote the start and finish of the recovery process, respectively)

network structure (Cimellaro et al., 2016). Figure 1 shows a schematic illustration of the WDN performance-based resilience quantification. At each time step, a performance metric is used to evaluate the current system state, which can be divided into the prior and post-hazard disturbance. For the post-hazard part, it can be further divided into the response stage (Stage II) and the recovery stage (Stage III). A common resilience quantified method is using the area under the curve as the system resilience index (SRI) as shown in the gray area of Figure 1.

The recovery decisions play an important role in the post-hazards WDN system performance recovery process or the WDN system resilience. As shown in Figure 1, the faster the system recovers from disruption, the larger area under the recovery performance curve (defined as SRI), the more resilient the system is. Different decision models have been proposed in previous research to improve decisions on WDN system restoration sequence. However, due to the complex hydraulic relationships in a WDN and the stochastic characteristics of failures, determining an optimal restoration sequence to maximize the system resilience remains a challenging problem. Different methods have been developed to find the optimal WDN restoration sequence, which can be grouped into (1) general-purpose metaheuristic algorithms, (2) greedy algorithms, and (3) ranking-based prioritizations (Paez et al., 2020).

The general-purpose metaheuristic algorithms define the problem of determining the optimal restoration plan as a global optimization problem, which is solved by using algorithms such as the genetic algorithm (GA), GA variants (NSGA-II), multi-objective evolutionary algorithm (Hosseini et al., 2016; Hossain et al., 2019; W. Liu & Song, 2020; Ouyang & Wang, 2015; Zhang & Wang, 2016). The

problems are often defined as an integer programming model (González et al., 2016; Nurre et al., 2012).

These algorithms, however, are computationally demanding and time-consuming. These make the general-purpose metaheuristic algorithms only suitable for pre-defined damage scenarios. Given the uncertainties associated with the exact damages during hazards, the high computational demand limits the applicability of this type of algorithms. Compared to the general-purpose metaheuristic algorithms, the greedy search-based method efficiently reduces the computing time (Castro-Gama & Quintiliani, 2018; W. Liu & Song, 2020). A greedy search method is a sub-optimal solution that selects the actions based on local optimization. For example, W. Liu and Song (2020) applied two greedy search methods for the WDN recovery based on the performance improvement at each time step. The effectiveness of the greedy search method has also been proved in the WDN optimal restoration problem (Cormen et al., 2009; Y. Liu et al., 2017; Pinzinger et al., 2011; Uber et al., 2004). Given its ability to achieve a decent performance with high computation efficiency, the greedy search algorithm is regarded as the most applicable method in the case of an emergency. However, the mechanism of this method can only achieve a sub-optimal solution. The ranking-based prioritization determines the restoration plan based on the ranking of the pipe importance. For example, Balut et al. (2018) ranked the pipe importance based on six criteria, that is, pipe diameter, distance from the source, velocity, flow, pipe closure impact, and so forth. The results indicate the diameter prioritized repairing sequence achieved better performance under most damage scenarios. Brink et al. (2012) compared four different restoration strategies based on experts' knowledge. W. Liu et al. (2020) applied a damage-based prioritization and prioritized the repairing strategy based on distance-to-source. The ranking-based prioritization method is fast since it does not require conducting any hydraulic simulation during the decision-making process. It relies on the list of pipes ranked by their relative importance, which is subjected to expert judgments.

The recent development in advanced machine learning (ML) provides civil engineers with more powerful tools for solving practical problems (Ahmadlou & Adeli, 2010; Alam et al., 2020; Pereira et al., 2020; Rafiei & Adeli, 2017). This paper explored a novel post-hazard recovery decision-support framework by integrating the graph convolutional neural network (CNN; GCN) into deep reinforcement learning (DRL) to determine the optimal WDN restoration sequence after the earthquake. The artificial intelligence (AI)-based decision support model is named the GCN-DRL model. The GCN-DRL model utilizes GCN to encode the topological information of the WDN and uses the DRL framework to learn and identify the optimal restoration sequence that maximizes the SRI during the recovery process. In principle, this method belongs to the general-purpose metaheuristic methods that solve the global optimization problem. However, the GCN-DRL model can take advantage of the transfer learning strategy, where the pre-trained GCN-DRL model can be extended for new disasters. This can significantly reduce the computational time for new damage situations, which is crucial for fast emergency responses.

The paper is organized as follows: Section 2 introduces the dynamic demand-based seismic resilience evaluation model, which consists of a model for assessing the damages of WDNs subjected to earthquakes, a model for WDN recovery, a model for WDN performance measurement, and a model for WDN resilience quantification. The resilience evaluation model is the key testbed as it allows to quantify the performance of different repairing sequences that are determined by different optimization methods. Section 3 starts with introducing the background of DRL and GCN. This is followed by the description of the detailed architecture of the proposed GCN-DRL ML model. Section 4 describes the application and performance of the proposed ML model for a widely used WDN testbed (Hernadez et al., 2016). The testbed is assumed to be subjected to different earthquakes so different damage situations can be generated. The final performance of different optimization methods under different seismic situations is also compared. Section 5 summarizes the major conclusions of this study and discussed future research needs.

2 | THEORETICAL FRAMEWORK FOR POST-EARTHQUAKE PERFORMANCE RECOVERY AND RESILIENCE ASSESSMENT OF WDN SYSTEM

The SRI, which is defined as the integration of the time-dependent system performance degree (PDW(t)) during the post-hazard recovery process, is utilized to measure the system resilience (i.e., Figure 1). In this study, WDN is assumed to be subjected to earthquakes. The performance of the WDN system is indicated by its capability to meet the water-use demands of customers after the earthquake. An analysis framework is developed for the WDN system seismic damage model, recovery model, and resilience assessment. Figure 2 shows the overall procedures to implement the proposed recovery-based resilience evaluation framework, which is used to evaluate the performance of different system repairing strategies. Details of these components are introduced in the subsequent sections. The overall procedures include.

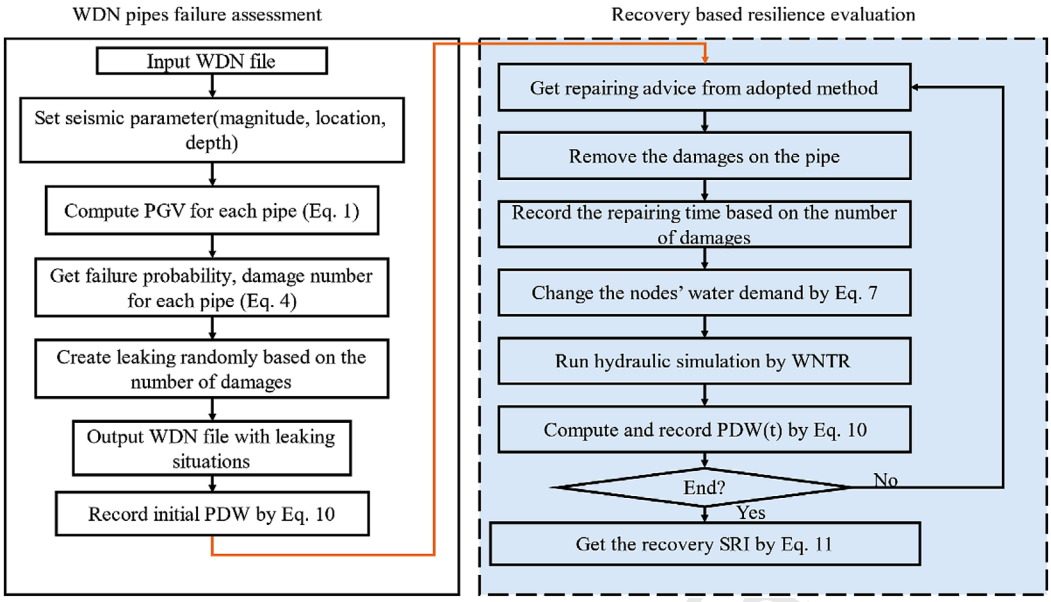

FIGURE 2 Illustration of framework of the system resilience assessment and recovery

1. A hydraulic model of the WDN is first constructed. This requires collecting the basic hydraulic information of the WDN needed for the hydraulic simulation, such as WDN topological connection structure, pipe length, water user demands, and so forth.
2. Then, the earthquake damages on the WDN are randomly generated based on the seismic vulnerability of the WDN. The damage here indicates the leakage point of each pipe. Thus, a pipe with a high failure probability may have more leakage points than that with a low failure probability. While a pipe with extremely low failure probability may have zero damage points. After determining the initial damage situation, a hydraulic simulation is conducted to obtain the initial performance degree of WDN (PDW) after the earthquake before the recovery stage begins.
3. The system recovery model includes components that consider the dynamic changing of user water demand, pipe repairment, and system performance evaluation. At each time step, a damaged pipe is selected for repair by the adopted repairing strategy. The repairing time for a pipe is assumed to be dependent upon the number of leakages along the pipe. Once repaired, the leakages on the pipe are removed for the selected pipe. The user's water demand is changed, and subsequently the hydraulic simulation is conducted. The PDW at each time step is determined based on the system performance evaluation indicator. The repairing process is repeated until all the damaged pipes are restored. The final SRI is determined (i.e., Equation 11).

To evaluate the performance of the developed GCN-DRL method (S1), the system recovery processes by this method are compared with four other methods for the repair strategies, including two greedy search-based methods (named S2 and S3; W. Liu et al., 2020), a GA method (S4; Zhang et al., 2017), and a diameter-based repair prioritization method (S5; Balut et al., 2018).

2.1 | WDN seismic damage model

Various components of WDN, including pipes, tanks, pumps, and water treatment facilities, could all be subjected to different extents of damages by earthquakes. To simplify the analyses without the loss of generality, this paper focuses on the repair sequence of distributed components, that is, pipelines. The localized facilities (i.e., tanks, pumps, and water treatment facilities) are not considered in the analyses. Similar assumptions were also used in previous studies (W. Liu et al., 2020). A number of studies about the WDN response to seismic have been proposed (Alliance, 2001; M. O'Rourke & Ayala, 1993). The American Lifeline Alliance model (Alliance, 2001) is one of the most commonly used models. Moreover, several studies extended this model by considering factors such as previous non-seismic records and pipe deterioration (Fragiadakis & Christodoulou, 2014). In this study, the damage model proposed by Mazumder et al. (2020) is used. The utilized damage model considers the relationship between peak ground velocity (PGV) and pipe repair rate to describe the pipe fragility curve. For the PGV estimation of an earthquake event, an empirical equation, Equation (1), proposed by Yu and Jin (2008) is adopted in this paper since it is

Material	k_1	k_c
Asbestos	1.0	1.0
Cast Iron	1.0	1.0~3.0
Ductile Iron	0.5	1.5
PVC	0.5	1.0
Steel	0.7	1.0

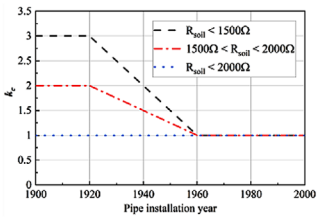

FIGURE 3 Parameters k_1 and k_c that consider the effects of pipe material, soil electrical electric conductivity, and pipe age (Mazumder et al., 2020)

developed with a dataset collected at a similar location to the testbed WDN of this study:

$$PGV = 10^{-0.848+0.775M-1.834\log(R+17)} \quad (1)$$

where R is the distance from the epicenter (km) and M is the magnitude of the earthquake.

With the information of PGV, the pipe failure probability with the consideration of pipe materials and deterioration by aging is determined by Equation (2):

$$P(f) = 1 - e^{-k_1 k_c{}^{*}0.00187^{*}PGV} \quad (2)$$

where $P(f)$ is the pipe failure probability every 1000 feet (304.8 m). k_1 is the correction factor by the pipe material, and k_c is are the correction factors that consider the effects of pipe material, size, soil type (electrical conductivity), and age (deterioration). The recommended values of k_1, k_c for different pipes can be found in the sub-table in Figure 3. k_c for cast iron is dependent upon the soil electrical conductivity and age.

Previous studies often use predefined damage status for each pipe, such as "leak" or "break," to describe the extent of damages. For example, Paez et al. (2018) used different emitter coefficients for leaks and breaks. This study simplified the treatment of the extent of damage by using different numbers of leakage points along the pipe based on its failure probability. The larger the number of leakages, the more the pipe behaves like "break" status and requires a longer time to repair. The occurrence of leak numbers along a pipe is assumed to follow Poisson's distribution (Cimellaro et al., 2016; Equation 3):

$$P(m) = \frac{\left(\lambda\left(\frac{L}{L_0}\right)\right)^m}{m!} e^{-\lambda\left(\frac{L}{L_0}\right)} \quad (3)$$

where $P(m)$ is the probability of m damages occurring in the pipe, L is the total length of the pipe, and L_0 is a reference length of 1000 ft (304.8 m).

The parameter λ of Poisson's distribution in Equation (3) can be estimated based on the probability where no failure occurs on the pipe by using Equations (4) and (5):

$$P(m = 0) = 1 - P(f) = e^{-\lambda\left(\frac{L}{L_0}\right)} \quad (4)$$

$$\lambda = -\frac{\ln(1-P(f))}{\left(\frac{L}{L_0}\right)} \quad (5)$$

To determine the consequence of a seismic hazard, the number of failure locations along each pipe is randomly sampled with the corresponding Poisson distribution (Equation 3). The position of a pipe failure is assumed to occur at a random location along a pipe.

The effects of seismic damages on the operation of WDN are simulated by assuming that the damages will cause leakages in the pipelines. In principle, the leaking sizes may vary with the extent of damages to the pipes. For simplicity, the damages are simulated as leaks with the same leakage model as shown in Equation (6). This, however, can be easily extended when more accurate information is available for a specific WDN. The seismic failure assessment of the water pipe network is coded by Python scripts:

$$d_{leak} = C_d A\sqrt{2gh} \quad (6)$$

where d_{leak} is the leakage water flow, A is the leakage area, C_d is the discharge coefficient, and h is the water pressure at the leakage point. In this study, the discharge coefficient is used 0.75 by assuming a turbulent flow (Lambert, 2001), and the leakage area A is selected based on an empirical equation $A = \pi^{*}0.25\%^{*}d^2$ (Shi & O'Rourke, 2008).

The hydraulic conditions of the WDN under normal operation and post-earthquake failure conditions are simulated by the hydraulic simulation solver WNTR (Klise et al., 2020). WNTR is an open-source python package for hydraulic simulations of the water pipe system, which solves similar sets of hydraulic equations as EPANET 2.2 (Rossman et al., 2020). By treating earthquake damages and repair as the proper boundary conditions, the water pressure at any location in the WDN can be determined. Q4

2.2 | WDN system recovery model

As only pipe damages are considered in the WDN system damage model, the only action at each timestep is

to decide which pipe should be repaired. However, more types of actions can be considered by extending this framework (such as close valve, pipe replacement, pipe inspection, etc.) as long as the influence on pipe hydraulic conditions and repair time are available. This study also considers the possible dynamic change of user's water demand during the recovery process. Didier et al. (2018) studied the post-earthquake water demand behaviors after the 2015 Gorkha Earthquake. The results indicated that the expected water demand decreased significantly when subjected to a high level of damages to buildings and equipment. Although the buildings and equipment restoration should be independent of the WDN restoration process, we assume the user-expected water demand is restored to the level before the earthquake, which is a simplification due to the lack of data. Specifically, a quadratic model is assumed to describe the time evolution trends of water demand post-earthquake, that is, disruption and then recovery process in Equation (7):

$$D_i^0(t) = \begin{cases} \left(\frac{t}{t_{\text{total}}}\right)^2 * D_i^0 & t > 0 \\ 0.0001 * D_i^0 & t = 0 \end{cases} \tag{7}$$

where D_i^0 is the expected water demand before the earthquake, t is the time step during the recovery process and $t = 0$ corresponds to the time when repair of pipes starts. It is assumed that users will still use a small amount of water even when the facilities are damaged at the beginning. $t > 0$ corresponds to the recovery period. t_{total} is the total recovery time, which is determined by the initial damage situation or the total number of pipe failures due to the earthquake hazard.

To consider the influence of water leakages, the pressure-dependent hydraulic model is adopted. The real-time water supply to each node on the WDN is determined by the expected water demand and the actual water pressure. The relationship between the real-time water supply (D_i) and the expected water demand (D_i^0) is shown in Equation (8) (Wagner et al., 1988). The hydraulic simulation is conducted at each time step after a selected pipe is repaired:

$$D_i(t) = \begin{cases} 0 & p_i < p_0 \\ D_i^0 \left(\frac{p_i - p_0}{p_u - p_0}\right)^{\frac{1}{2}} & p_0 \le p_i \le p_u \\ D_i^0 & p_i > p_u \end{cases} \tag{8}$$

where p_i is the actual water pressure at the node, p_0 is the predefined lower bound of water pressure (under which no water is supplied), p_u is the upper bound of water pressure (the minimum pressure to ensure water supply to meet the design water demand). p_0 and p_u are set as 0 and 30 m as recommended by Zhou et al. (2019).

To focus on the key problem without loss of generality, the following assumptions are made in developing a decision support model for the optimal repair sequence to restore the WDN service.

1. *Repair time for pipe damages*: Different types of damaged pipes may require different repairing times. For example, the Federal Emergency Management Agency provided the estimated repairing time of different WDN components (Federal Emergency Management Agency, 2003). To simplify the analyses, it is assumed an equal amount of time is needed to fix a leakage point in a pipe. With this assumption, the repairing time of each pipe is determined by the total leakage locations alongside this pipe. The number of leakages along a given pipe is affected by the pipe material, age, soil type, location, and uncertainty (i.e., Poisson distribution; Equations 3–5).
2. *Binary working status of damaged pipes*: The typical pipe repairing process involves closing the pipe end connections. A damaged pipe is re-open only when all repairs along this pipe are finished. This study assumes that a damaged pipe is either closed (when damaged) or open (when repaired) based on the status of the repair. This assumption simplifies the hydraulic model of the WDN.
3. *Resource for repair*: A single repair team is assumed, that is, the WDN is repaired with one repairing team with no resource limits. No parallel repairs by multiple teams are considered. This is also a common assumption used in prior research in determining the optimal recovery sequence of WDN (Almoghathawi et al., 2019; W. Liu et al., 2020). This assumption ensures the failed pipes are recovered sequentially one by one. However, it is noted that more sophisticated assumptions on the number of repair teams and their work efficiency can be incorporated.
3. *Non-preemptive recovery*: It is assumed that the repairing team has to finish the repairing work on the current pipe before moving to repair the next pipe. This assumption is often used in analyzing infrastructure repair processes such as roads, bridges, and power grids, and so forth.
4. *Dynamic changing post-earthquake water demands*: The water demand at each node of WDN is assumed to gradually restore to the pre-hazard condition as the restoration of WDN continues. A single post-hazard dynamic water demand recovery process is used in this study. It is noted that different nodes in the WDN could experience different dynamic water demand restoration process depending upon the function and location of the nodes. However, multiple dynamic water demand patterns can be easily added when such data is available.

2.3 | WDN system performance evaluation model

The performance of the WDN is measured by its capability to meet the customers' water use demands. Given the essential role of clean water supply to public life, it should also be one of the most important criteria for post-hazard restoration decisions (Romero et al., 2010). The water-user nodes satisfaction degree (NSD) is used to quantify the performance of the system in this study. The NSD is defined as a ratio of the expected water use at the node and actual water supplied to the node (Equation 9). NSD value larger than 1 is assumed to be 1 (or water demand at the node is fully met). The NSD is defined as follows:

$$NSD_i\ (t) = \begin{cases} 1 & D_i\,(t) \geq D_i^0\,(t) \\ \frac{D_i(t)}{D_i^0(t)} & D_i\,(t) < D_i^0\,(t) \end{cases} \tag{9}$$

where $D_i(t)$ is the actual water supply to the node at t and $D_i^0(t)$ is the expected post-earthquake water demand at t. The units of both two variables are flow rate (m^3/s).

Based on the NSD defined for each node, the overall degree of performance of a complete WDN is defined as the performance degree of the water network, which is calculated as the weighted sum of the NSD at each node in the WDN (Equation 10). The weight factor considers the relative importance of the node. Using NSD to measure the overall WDN performance allows considering the importance of critical water supply nodes by assigning appropriate weight to the nodes (i.e., Equation 10). For example, restoring water supply to critical facilities such as hospitals, firefighting stations, schools, and so forth is more critical than less safety critical facilities. The important nodes can be prioritized in the restoration plan by assigning proper weights to the NSD, which can be considered for the seismic consequence analysis (Shahata & Zayed, 2016):

$$PDW\ (t) = \sum_{i=1}^{n} w_i{}^{*} NSD_i\,(t) \tag{10}$$

where $NSD_i(t)$ is the node satisfactory degree at time t that belongs to $(0, 1]$ and w_i is the weight factors that consider the relative importance of the nodes ω_i; the weight factor for each node i is calculated by $w_i = \frac{\omega_i}{\sum_{j=1}^{n} \omega_j}$, where n is the total number of service nodes. The weight of a node w_i should be subjected to $\sum_{i=1}^{n} w_i = 1$. Therefore, the PDW at any time t falls within the range $[0, 1]$.

As some prior studies indicated, the weight or importance of a water supply node may also change during the restoration process. A detailed method to quantify the importance of different nodes is out of the scope of this study. A pre-defined fixed weight for each water supply node is used in this paper. Dynamic changing of node importance can be considered by using the proposed framework, which is similar to the consideration of the dynamic changing of user's expected water demands.

2.4 | WDN system resilience index and resilient restoration

Based on the definition of the $PWD(t)$ (Equation 10), the SRI during the recovery process is defined using the area of under-recovery curve of $PWD(t)$ (Figure 1), that is, Equation (11):

$$\mathrm{SRI} = \int_{t_0}^{t_{\mathrm{end}}} PDW\,(t)\,dt = \sum_{t=t_0}^{t_{\mathrm{end}}} PDW\,(t) \tag{11}$$

where t_{end} is the time of ending recovery, t_0 is the time of beginning recovery; the integration is normalized by $(t_{\mathrm{end}} - t_0)$ to consider the effects of recovery time.

To obtain a resilient restoration plan, the repairing sequence of damaged pipes is expected to achieve a higher SRI value at the end of the recovery process. In this study, we use the SRI function (Equation 11) as the only optimization objective. Although previous studies used different standards for recovery evaluation (Paez et al., 2018), the problem can still be taken as a single objective optimization problem by assigning appropriate weights to each standard.

To obtain a resilient restoration plan, the repairing sequence of damaged pipes is expected to achieve a higher SRI value at the end of the recovery process. In this study, the SRI value is set as the optimization goal (i.e., maximization of SRI by proper decision sequence). It is noted that some of the previous studies used different measurements of the recovery-based system resilience, and these resilience measurements can be easily adapted as the optimization goal.

2.5 | Optimal restoration problem

Given the aforementioned description of the seismic damage model, recovery model, and evaluation model, the efficiency of different decision-making methods can be easily quantified by using the SRI value (Equation 11). Hence, the optimal restoration problem in this study can be defined as finding the most optimal repairing sequence that can achieve the highest SRI value. Mathematically, the

problem of optimal repairing sequence is defined in Equations (12) to (14). Equation 12 defines the main objective function for optimization, which aims to maximize SRI given a decision vector a. The decision vector is the repairing decision at each time step, that is, $(a_0, a_1, \ldots, a_{t_{\text{end}}})$. Equations (13) and (14) define the constraints when solving the optimization problems, that is, the repairing decision at each time step should not be repeated, and the union of repaired decisions should equal the set of damaged pipes:

$$\text{argmax SRI}(a) \tag{12}$$

s.t.

$$a_1 \neq a_2 \neq a_3 \ldots \neq a_{t_{\text{end}}} \tag{13}$$

$$a_1 \cup a_2 \cup a_3, \ldots \cup a_{t_{\text{end}}} = \text{K} \tag{14}$$

where $SRI(\cdot)$ is the resilience of WDN with the given repairing sequence a, a_t is the selected pipe for repairing in time step t, and K is the set of damaged pipes due to the hazards.

3 | GCN-DRL MODEL

3.1 | DRL and GCN

3.1.1 | DRL

DRL is an impactful development in ML model. It provides a powerful new approach to solve optimization problems based on a series of actions. DRL achieves promising results to identify the optimal action sequence from a massive set of action spaces and based on the corresponding system states and interactions with the environment. Andriotis and Papakonstantinou (2019) provided a detailed introduction about the successful DRL applications in the management system. DRL has also been successfully applied in areas such as vehicle control (Y. Wang et al., 2020) and pavement maintenance (Yao et al., 2020), which have proven the ability of DRL for global optimization problems with high efficiency.

For the WDN restoration, the problem of optimal repair sequence is a global optimization problem. A decision-maker is expected to decide which pipe should be repaired under the current system state and then make the next decision based on the next system state. This problem can be illustrated in Figure 4; at each time step, the agent makes a decision on which pipe should be repaired, that is, a_i, from the defined action space K (the set of damaged pipes). This action changes the system state from s_i to s_{i+1} as the NSD of each point changed due to this repairing action. In the meanwhile, the system will feedback a reward r_i to reward the agent based on how good this action is to positively change the system state. To achieve a global optimal repairing sequence, the agent should not only consider the instant reward of each action but also consider its potential influence in the future. However, such a decision-making process is extremely challenging for humans as the influence of current decisions on the future is hard to be quantified. To overcome this challenge, the reinforcement learning (RL) algorithm is utilized to evaluate the performance of each action based on its instant reward and future reward.

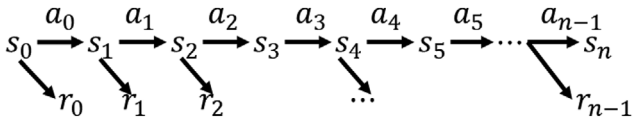

FIGURE 4 Illustration of Q-learning (Note: $s_t \in S$ is the states of the system, $a_t \in K$ is the space of action, r_t is the reward of action a_i when the station is s_t)

Unlike the greedy search-based method that only computes the instant reward, RL gives a Q value to each action under different system states. In this study, the system state is represented by the NSD value considering the system topological structure. According to the theory of RL, the Q value integrates the action's instant reward and the max Q value of the next state after taking this action. Such a Q value is defined as the Bellman equation (Bellman, 1952) as shown in Equation (15). As demonstrated by (Mnih et al., 2013), by iteratively sampling all the actions under all the states, the RL model will compile the Q values of each action under each state to get a Q table. Then, the RL model determines the most optimal action by choosing the action with the highest Q value:

$$Q(s,a) = \mathbb{E}[\underbrace{r}_{\substack{instant\\reward}} + \gamma \cdot \underbrace{\max Q^*(s', a^*)}_{optimal\ future\ reward}] \tag{15}$$

where the $\mathbb{E}$ denotes the expectation of Q value (Sutton & Barto, 2018), r is the immediate reward after taking action a, and γ is the return discount for future rewards by following optimal policy of next state s_{i+1}. $Q^*(s', a^*)$ indicates the Q values of all the actions at next state s'.

However, for most real-world problems, the aforementioned Q table is extremely hard to obtain due to the infinite number of combinations of states and actions. For the WDN restoration problem, 50 damaged pipes could lead to 50! possible restoration sequences. To overcome this

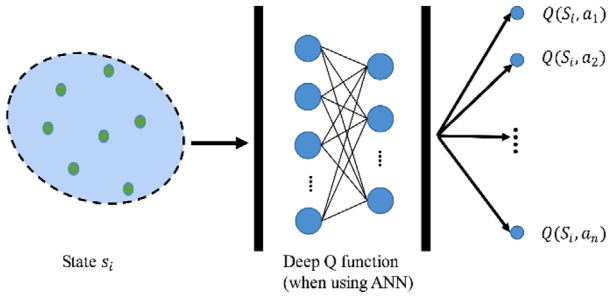

FIGURE 5 Illustrative concept of deep reinforcement learning (DRL) that uses artificial neural network as the Deep Q function

challenge of searching for the optimal action from an infinite large action space, DRL is proposed. The DRL intends to leverage the advancement in deep learning to solve the traditional RL problem Mnih et al. (2013) as shown in Figure 5. Moreover, a deep Q function is utilized to estimate the Q value of each action based on the current system state. Hence, such a Deep Q function should have the ability to interpret the current system state and approximate the Q value of each action. Traditional DRL typically uses common types of artificial neural networks (ANN) as the Deep Q function. However, the ANN models typically use a tabular- type of input data. They are not effective when dealing with graph type of data such as the data from infrastructure networks. To further advance this domain, a GCN is incorporated in this study to be the Deep Q function to encode the network structure of WDN and the corresponding data.

3.1.2 | GCN

The GCN was first proposed by LeCun et al. (1998) as inspired by the motivation of the CNN (Guo et al., 2020, 2021; Jeong et al., 2020; Tang et al., 2021; F. Wang et al., 2021). Graph neural network is a special neural network that can directly operate on graphic structural data. The GCN utilized the key ideas of a CNN, such as local connection, shared weights, and the use of multi-layers. It, however, convolves the neighborhood's feature of each node, which overcame the limitation of CNN that can only perform on regular Euclidean data such as image (2D) and text (1D). In the civil engineering area, GCN has been applied for traffic flow prediction by treating the traffic network as a special type of graph (Li et al., 2017) and traffic control (Chen et al., 2021). The successful applications of GCN in different domains have proven the potentials of GCN in understanding the complex relationships in a graph structure.

In the decision-making process, understanding the relationships in the current graph structure plays the most important part when targeting a global optimization. However, unlike some local optimization methods, there is no determined mathematical equation that can be used in this process. The neural network provides a novel approach to mimic human neural activity. By integrating the GCN-DRL and WDN recovery model, the parameters inside the GCN can be trained to mimic the expert's experience and intuitive accumulation process to obtain a global optimization decision. Specifically, the input of the GCN is the current state of WDN, including the WDN structure (including pipe length and connection matrix), and the satisfactory degree of each node (Equation 9). The output of the GCN is a matrix of vectors that represents the understanding of the current WDN by the GCN. Such output is difficult to be interpreted but it will be transformed into a list of action scores by the following neural network layer. The process is introduced in the following section.

In this paper, the GCN implemented by Kipf and Welling (2016) is utilized for WDN network analysis. The layer of GCN performs a convolutional process on a graph-structured dataset. Unlike the traditional 2D convolutional process of CNN, which focused on extracting the feature via a selected convolution filter, the GCN layer conducts the feature extraction of each vertex and its neighbors. Therefore, the structure of the graph is considered. Mathematically, a graph convolutional layer in GCN will project the nodes of the WDN network into a latent space by using Equation (16):

$$H^{l+1} = \sigma\left(\tilde{D}^{-\frac{1}{2}}\tilde{A}\tilde{D}^{-\frac{1}{2}}H^{l}W^{l}\right) \tag{16}$$

where H^l is input to the lth layer of GCN neural network. At the input layer $l = 0$, $H^0 = X$, where X is the feature matrix of the graph whose dimension is $N \times D$, N is the number of nodes, D is the number of features of each node; $\tilde{A} = A + I$, where A is the representative description of the graph structure. An adjacency matrix is used in this study to describe the graph structure. I is the identity matrix with the same dimension as A; $\tilde{D}$ is the diagonal node degree matrix of $\tilde{A}$; $\sigma(\cdot)$ denotes the activation function. The commonly used ReLU activation function is used in this study; W^l is the weight matrix of the lth layer.

The input to the GCN is the feature matrix of the graph, $\mathbf{X}$, whose dimension is $N \times D$, N is the number of nodes, D is the number of features of each node. In this study, one feature is used for node attribute, which is the NSD defined in Equation (9). The output of the GCN is a matrix that contains the embedding information of the current WDN by the GCN. Each row of the matrix represents the latent space value of each node. The number of rows equals the number of total nodes in the WDN.

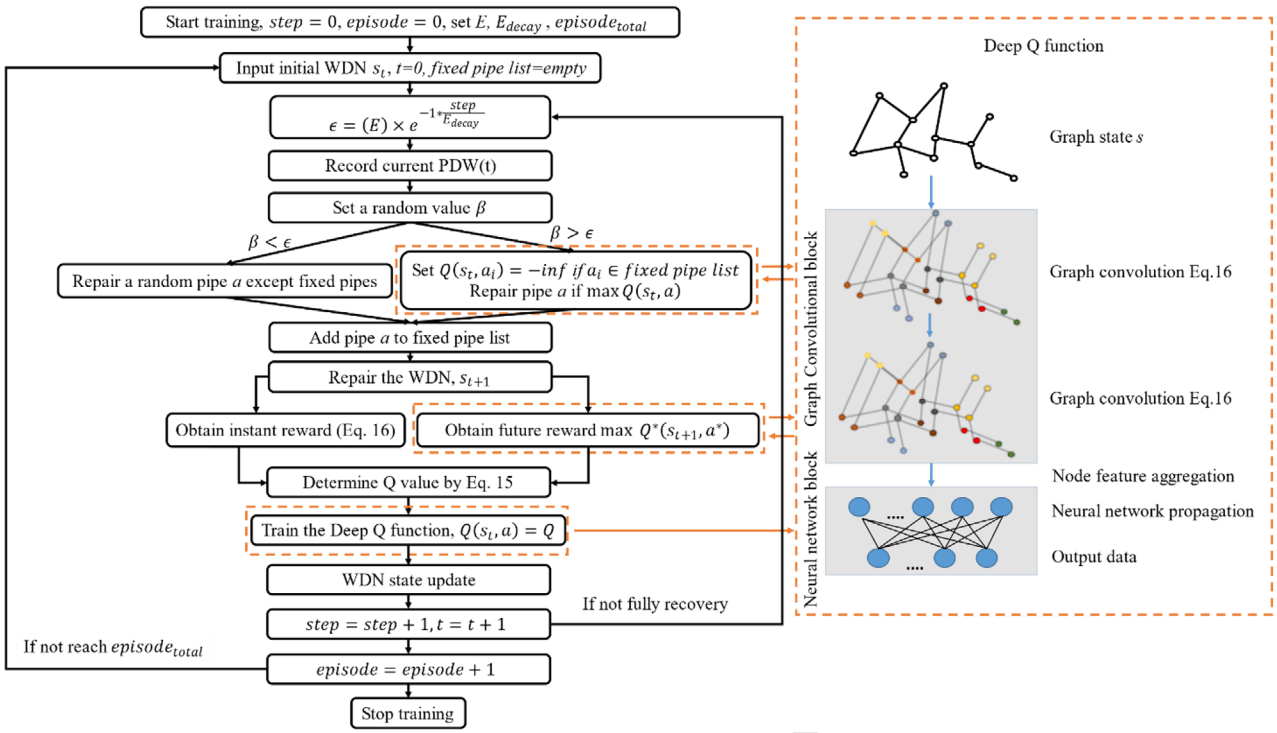

FIGURE 6 The architecture of graph convolutional neural network-DRL hybrid machine learning model (*step*: record current training times, *episode*: one recovery revolution, E: initial value of ϵ, E_{decay}: decay rate of ϵ during the training process, $episode_{total}$: total training revolutions, s_t: WDN state at time t, β: random value, and a: pipe ID for repairing)

3.2 | Proposed GCN-DRL model

A GCN-integrated DRL (noted as GCN-DRL) model is proposed in this study to optimize WDN recovery by combining the GCN and DRL. Recent studies have also proved the power of using GCN and DRL in different areas such as radio networks (Zhao et al., 2020), virtual networks (Yan et al., 2020), and manufacturing systems (Hu et al., 2020). This study is the first attempt to integrate GCN and DRL to extract information from the WDN and make optimal decisions for post hazards restoration.

The architecture of the proposed GCN-DRL model is shown in Figure 6. The left side of Figure 6 illustrates the reinforcement training framework (DRL) to train the Deep Q function, and the right side of Figure 6 provides the architecture of the proposed Deep Q function that integrates two GCN layers and one neural network layer. The framework is illustrated as follows:

1. At the beginning stage, the parameters that are used to control the training process should be initialized, that is, the E, E_{decay}, and $episode_{\text{total}}$. The first two parameters are used to determine ϵ. This ϵ is used to control the probability of "taking actions randomly" and "taking actions based on Deep Q function," which is also known as epsilon-greedy policy (Wiering & Van Otterlo, 2012). The benefit of taking random actions is that this process could prevent the agent from being trapped by the local optimal solution especially when its experience is limited.
2. A fixed pipe list is also initiated to record fixed pipes. This list is used to prevent any pipes from being repaired repeatedly. As shown in Figure 6, a pipe is either randomly selected from the remaining failure pipes or determined based on the Deep Q function. In this study, the output of the proposed Deep Q function is a list of repairing scores. Hence, the pipe with the highest repairing score will be selected. This is the first time interaction between the deep learning framework and the Deep Q function as shown by the top arrow in Figure 6.
3. The WDN is repaired based on the selected pipe. Consequently, the hydraulic situation of the WDN is changed. The supplied water of each node is recalculated by running the hydraulic simulation (Section 2.2), in which the next state s_{t+1} of the WDN is obtained.
4. Two reward values are essential to determine the award score (Q) of each action, that is, the instant reward function and the future reward function (Equation 15). In this study, the instant reward is set proportional to the

improvement in the PDW with the consideration of repairing time (Equation 17). The WNTR model is used to calculate the PDW of the current state and one-step forward stat. The future reward is obtained by feeding the updated state of WDN into the Deep Q function to get the maximum output. This is shown by the middle arrow in Figure 6.

5. After obtaining the instant reward r_i and potential future reward (max $Q^*(s', a^*)$), the Q value of the selected action will be computed by Equation (15). Then it is fed back to the Deep Q function to train the inside neural networks. While such future reward is inaccurate at the beginning, However, with the training process development, this predicted value will be closer to the real Q function. This process is shown by the bottom arrow in Figure 6.
6. The training process will be repeated with a number of $episode_{\text{total}}$. Each episode denotes a full recovery revolution that contains a trial repairing sequence. The WDN state is also updated whenever an action is made. This trial-and-error process can be seen as a process mimicking an export accumulating the experience. For each integration, the parameters of the neural networks are calibrated and updated by the backward propagation process.

The integrated Deep Q function is shown on the right side of Figure 6, which contains two layers of GCN and two layers of ANN. As the output of the GCN layer is a matrix of $N \times D$ (refer to Equation 16), it cannot be directly fed into the following ANN layer. Inspired by CNN, we averaged the node values into a 1D vector space and then fed it into the ANN layer.

The detailed architecture of the Deep Q function emulated by the GCN is described as follows. The input to the Deep Q function is the WDN state, which is a graph structure data represented by the network structure and NSD. It is projected by the first graph convolution layer with 64 dimensions. The outputs are then projected to 128 dimensions by the second GCN layer. The output of the second GCN layer is aggregated by taking the average values of the projected node attribute in each dimension, which is 128 dimensions as well. Then this vector is fed into a neural network. The first layer of the neural network contains 128 neurons to accept the input data of 128 dimensions. The number of neurons in the second layer or the output layer of the neural network equals the dimension of the action space, which is the total number of initially damaged pipes. A linear activation function is used in the last layer of the neural network:

$$r = \frac{PDW_i(t) - PDW(t-1)}{T_i} \tag{17}$$

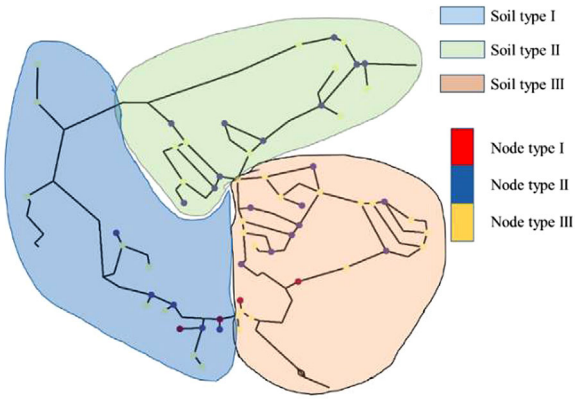

FIGURE 7 The testbed WDN of Fairfield, California, with annotation of node importance and ground soil types

where $PDW_i(t)$ is the degree of performance of WDN after taking repair action i, $PDW(t-1)$ is the degree of performance of WDN after previous repair action, and T_i is the duration needed in repairing pipe i. This study assumes that the repairing time is determined by the number of leakages in the damaged pipe.

The proposed GCN-DRL model is used to determine the pipe repair sequence. To achieve a smooth and stable training result, the technique "experience replay" described by Mnih et al. (2015) is also used in this study. The graph neural network and RL used in this study is implemented by the python deep graph library (M. Wang et al., 2019) and PyTorch library (Paszke et al., 2019).

4 | CASE STUDY

4.1 | Case study Rancho Solano Zone III WDN

The GCN-DRL-based repair decision-making model based on the recovery-based WDN seismic resilience evaluation framework is applied to analyze the seismic recovery of a testbed WDN located in Fairfield, California. The complete dataset about this WDN is publicly available from the database maintained by the University of Kentucky (Hernadez et al., 2016). The original water demand and water supply conditions are used in the study. The influence of pipe ages, materials, customer importance, and soil types is also considered in this case. The detailed information about the testbed is summarized in Table 1. The WDN structure, levels of node importance, and the soil types are shown in Figure 7. These attributes of each pipe and the seismic PGV are used to obtain the damage probability of each pipe.

TABLE 1 Summary of the information about the testbed

	Variable name	Value	Description
Water distribution network (WDN) structure	Number of pipes	126	Total number of edges
	Number of nodes	112	Total number of vertices
	Node elevation (above sea level; m)	[90, 139]	This is predefined by the dataset
Pipes	Pipe length (m)	[90, 1200]	This is predefined by the input file
	Pipe age (years)	[50, 100]	Randomly assigned to each pipe based on uniform distribution
	Pipe material	"ast iron," "ductile iron," "steel," "pvc," "asbestos"	Randomly assigned to each pipe
Customers	Number of customers	63	Vertices whose basic water demand is larger than 0
	Weights of customers (unitless)	I: $\omega = 5$ II: $\omega = 3$ III: $\omega = 2$	Different types of customers. I denotes the most important node and III denotes the least important
Soil	Soil type	I: $R_{soil} < 1500\ \Omega$ II: $1500\ \Omega < R_{soil} < 2000\ \Omega$ III: $R_{soil} > 2000\ \Omega$	Different types of soil, R_{soil} denotes the soil electrical resistivity. Distribution of soil type is shown in Figure 7

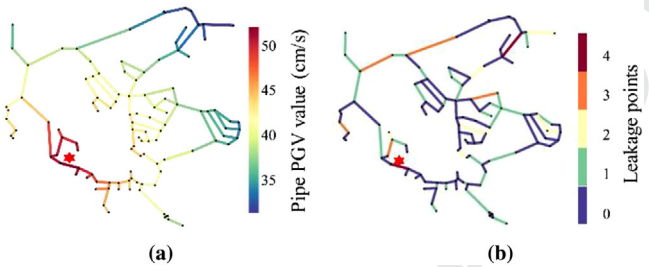

FIGURE 8 (a) Distribution of peak ground velocity (PGV) along the pipelines (cm/s); and (b) number of leakage points alongside the damaged pipe (see Supplementary materials)

4.2 | Water pipes seismic failure prediction and GCN-DRL hybrid model training

The WDN is first assumed to be subjected to a magnitude 6.5 earthquake with the epicenter located at the left bottom of the WDN (red star annotated in Figure 8). The depth of the earthquake is assumed to be 5 km. The earthquake-induced PGV is calculated using Equation (1) and shown in Figure 8a. The corresponding numbers of pipe damages are determined considering the influences of pipe material, pipe age, pipe length, and soil material based on the equations described in the earlier context (Equations 1–5). The final number of damages on each pipe is shown in Figure 8b. In summary, the earthquake causes 69 total damages points affecting 44 pipes. The initial PDW immediately after the earthquake is computed to be about 0.00564.

The proposed GCN-DRL model is trained to repair the damaged pipes in the WDN according to the framework described in Section 3.2. Table 2 shows the key parameters used in training the GCN-DRL mode. The total episode of training (or the number of complete repair sequences) is set as 500. Since 44 pipes are damaged, this means the Deep Q function is trained 22,000 times. The parameter ϵ, which determines if repair is by random decision or by RL learning, started with $\epsilon = 1$ and continues to decrease to a small value with progress in WDN repairment. The E_{decay} is set as 5000 so the ϵ value could be nearly 0 at the end of training (0.0122).

Figure 9 shows the SRI of the WDN system under 500 training episodes and the corresponding ϵ values. The smoothing SRI is derived from Savitzky–Golay filter (Schafer, 2011) as shown by the dashed line. The control parameter ϵ determines if the repair decision is made

TABLE 2 Key parameters used for the graph convolutional neural network integrated deep reinforcement learning model

Parameter	Description	Value
ϵ	The parameter controls the probability of action taken by randomly or GCN-based	$\epsilon = E \times e^{-1\times\frac{step}{E_{decay}}}$
E	The initial value of ϵ	1
E_{decay}	ϵ decay rate	5000
$episode_{total}$	Total revolution number for training. One episode means one complete recovery process	500

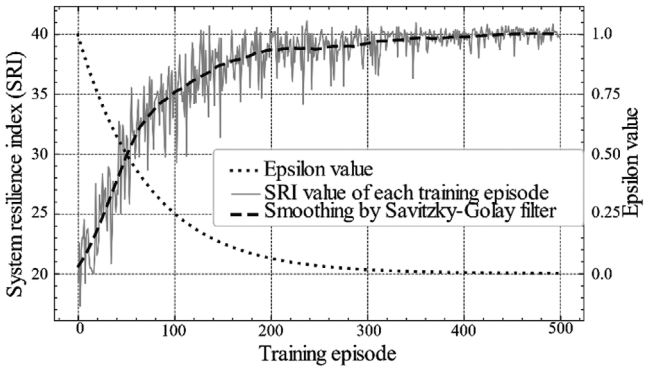

FIGURE 9 Illustration of the learning curve of proposed methods

randomly (large ϵ) or from the Deep Q function (small ϵ). The results imply that the SRI values in the first 70 episodes are relatively low and unstable since the control parameter ϵ is relatively large, these restoration actions are mainly randomly chosen (Figure 9). As the training process continues, the control parameter ϵ decreases, so the probability of taking actions guided by GCN increases. The agent makes decisions mostly based on the GCN after around 350 episodes, which achieved stable solutions with high SRI values. The fluctuations of the SRI are due to the inherent randomness of the neural networks and the high dimensional state space.

4.3 | Conventional decision-making methods for pipe recovery sequence

The performance of the repair sequence by the GCN-DRL ML model is compared with four conventional decision-making methods, including two greedy search-based strategies (S2 and S3; W. Liu et al., 2020), a GA method (S4; Moscato, 1989; Zhang et al., 2017), and a diameter-based repair prioritization method (S5; Balut et al., 2018). Although other repairing methods have been used in the previous studies, most of the methods belong to these classes and are different variants of these four methods. The detailed mechanisms of these conventional methods (named as S2 to S5) are briefly described as follows:

4.3.1 | S2: Static importance-based method

This method prioritizes pipe repair based on ranking the improvements of the PDW after repairing the pipe over the initial damaged status. The larger the ranking factor, the higher the priority for the pipe to be fixed. The ranking factor of pipe i is defined as

$$I_{s,i} = \frac{PDW_i - PDW_0}{T_i} \tag{18}$$

where PDW_i is the PDW after repairing pipe i, PDW_0 is the PDW before any recovery, and T_i is the repairing time for pipe i, which equals the number of damages on the pipe.

4.3.2 | S3: Dynamic importance-based method

This method determines the pipe repair priority by the dynamic importance during the recovery of the WDN. Unlike S2 that only compares the performance improvement with the initial damage status, S3 compares the performance between the pipe recovery and current WDN state by the following equation. The importance of pipe i is ranked based on $I_{d,i}(t)$

$$I_{d,i}\ (t) = \frac{PDW_i(t) - PDW(t-1)}{T_i} \tag{19}$$

where $PDW_i(t)$ is the PDW at time t after repairing pipe i, $PDW(t-1)$ is the PDW before the last time step, and T_i is the repairing time for pipe i, which equals its damage number.

4.3.3 | S4: GA-based method

GA is a global optimization algorithm. As a combinatorial optimization problem, the crossover method proposed by Moscato (1989) is used in this study as shown in Figure 10. First, a random subset of Parent 1 is selected and filled into the sequence in Parent 2. The mutation of each individual is performed by randomly exchanging two genes with

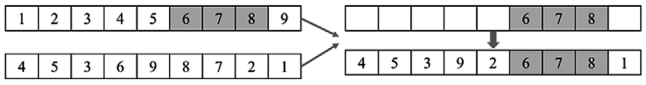

FIGURE 10 Illustration of crossover

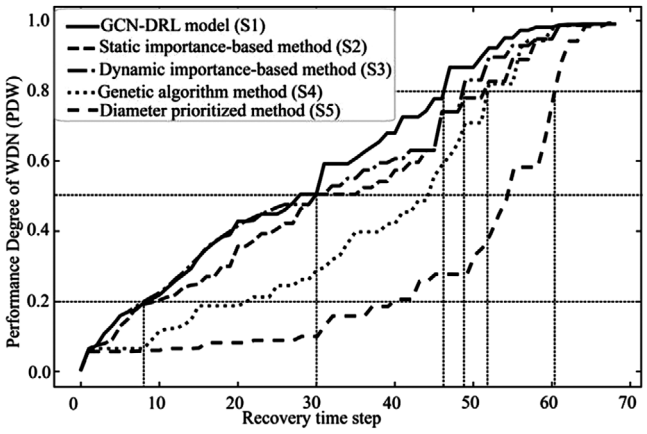

FIGURE 11 Trajectories of WDN recovery using repair sequences by different decision methods (i.e., S1 to S5)

TABLE 3 System resilience index (SRI) and computing time among different recovery methods

Method	S1	S2	S3	S4	S5
SRI	41.67	36.977	39.225	30.868	26.464
Time	2.3 h	3 min	15 min	3.2 h	2 min

a very low probability. In this study, this probability is set as 0.03.

4.3.4 | S5: Diameter-based repairing prioritization method

This method determines the repair sequence based on the ranking of the pipe diameter. The damaged pipes will be ranked based on the size of their diameter. The repairing sequence follows this ranked sequence.

4.4 | Evaluation of the computational performance

The computational performance of each method is evaluated by the final SRI value of the recovery trajectory, the recovery time to achieve a satisfactory level of system performance, and the computational time.

The recovery trajectories by using methods from S1 to S5 are shown in Figure 11 and the corresponding SRI values are summarized in Table 3. Compared with conventional methods (S2 to S5), the proposed GCN-DRL method (S1) improves the area under the trajectory curve, which corresponds to a higher SRI value. It is noted that the GA-based method (S4) is also a general-purpose metaheuristic method. The under-curve area of the recovery process by GCN-DRL (S1) is much larger than that by the GA method (S4) even when the GA method used two times the number of trials. This result indicates the GCN-DRL outperforms the GA as a global optimization method for repair sequence.

The recovery time to achieve a satisfactory level of system performance is critical for infrastructure restoration. Figure 11 also shows the recovery time to achieve certain performance levels of WDN based on repair sequences by different decision methods. The results imply that the repair sequences by S1, S2, and S3 achieved 20% and 50% performance degrees in a similar amount of time. After that, the repair sequence by the GCN-DRL (S1) method ensures the fastest recovery until the system is completely restored. The observations are attributed such that the developed GCN-DRL model (S1) can efficiently consider the future impact of repair decisions, compared to greedy search methods (S2 and S3) and therefore achieve a global optimal repairing sequence. The performance of the GA method (S4) lagged until the system recovers to about 95% of its original performance. Assuming 80% system performance is a satisfactory level, the proposed GCN-DRL method (S1) achieved around two time-steps ahead of S3 and around five time-steps ahead of GAs (S4). These demonstrate the superior performance of the GCN-DRL model in determining the optimal repair sequence, compared to conventional methods.

The computational time to determine the repair sequence by methods S1 to S5 is also shown in Table 3. The GCN-DRL ML model takes more computational time than S2, S3, and S5 since a large number of training iterations are involved. For example, in this case, the GCN-DRL model takes 500 training episodes, each training episode contains 44 times of repairing process (44 damaged pipes). Therefore, 22,000 hydraulic simulations were conducted to capture the WDN performance. The Deep Q function was also trained 22,000 times.

To further demonstrate the robustness of the developed method, two additional earthquake scenarios with different epicenters or magnitudes are considered, named as the second scenario and the third scenario. The second earthquake scenario is a magnitude 6.75 earthquake close to the center of the WND map, which caused 59 pipes to be damaged with 107 leaking locations. The third scenario is a magnitude 7 earthquake occurring at the top right, which caused 73 pipes to be damaged with 151 leaking locations. The initial PGV values and the corresponding water pipe damages under these two seismic scenarios are shown in Figure 12. The same parameters, that is, pipe material, age,

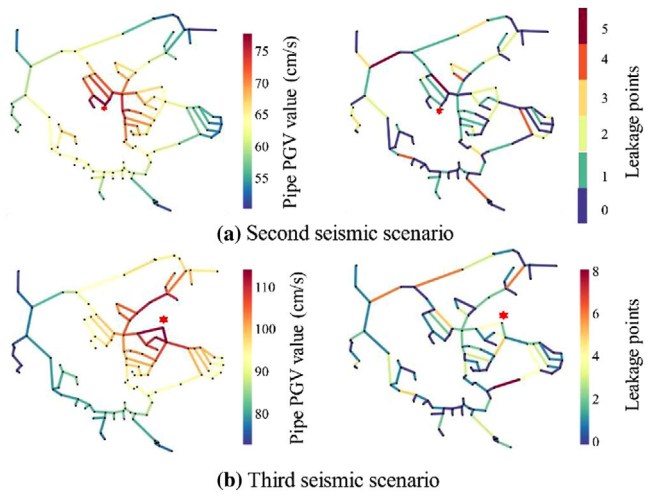

FIGURE 12 The initial PGV values and water pipe damage distributions under the second and third earthquake scenarios (see Supplementary material)

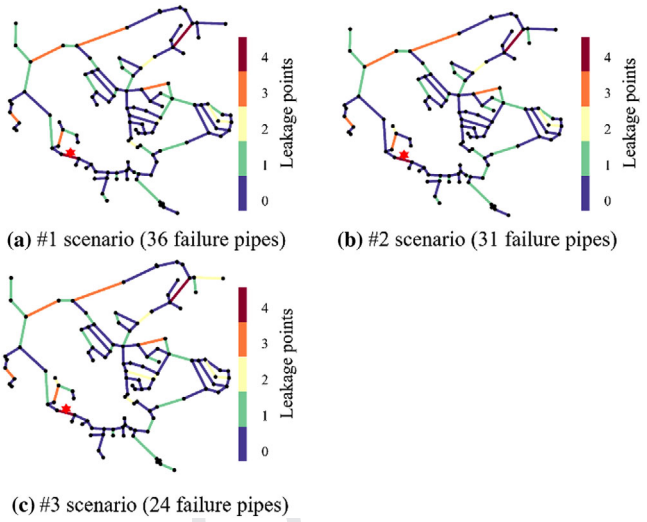

FIGURE 14 New failure situations as a subset of original failure pipes

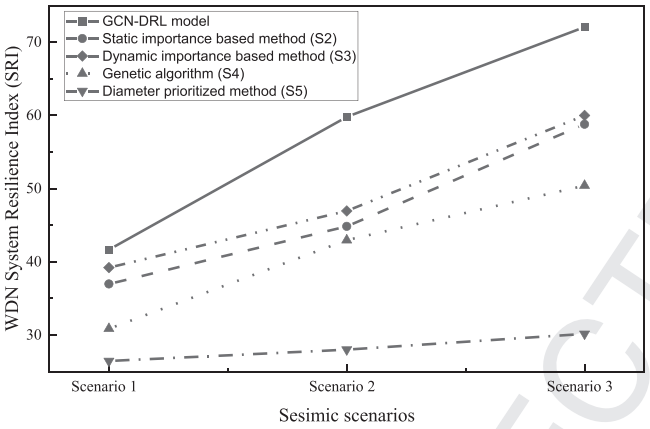

FIGURE 13 The final system resilience index values by different decision methods under different earthquake scenarios (Scenario 1: 44 pipes damaged with 69 leakages, Scenario 2: 59 pipes damaged with 107 leakages, Scenario 3: 73 pipes damaged with 151 leakages), Scenario 2: 59 pipes damaged with 107 leakages, Scenario 3: 73 pipes damaged with 151 leakages)

soil type, and consumer importance as the first seismic scenario are used in the damage and recovery analyses.

The final performance of system resilience, indicated by the final SRI values, of different repairing decision methods to recover from these three earthquakes, is summarized in Figure 13. As can be seen, the GCN-DRL model consistently outperforms the other decision methods for all these earthquakes. It is also noted that the more severe the earthquake damages, the more significant the GCN-DRL model improves the final SRI values. Or the more benefits in improving system resilience via globalized optimal decisions with the GCN-DRL model. Besides, compared with the other global optimization method, that is, the GA model, the GCN-DRL model is much more computationally efficient.

4.5 | Transfer learning for rapid responses

As pointed out by Paez et al. (2020), the general-purpose metaheuristic algorithms require high computational demands. These make the general-purpose metaheuristic algorithms only suitable for pre-defined damage scenarios. Given the uncertainties associated with the exact damages during hazards, the high computational demand limits the applicability of this type of algorithms. A novel transfer learning strategy is explored for the GCN-DRL for new disaster scenarios. That is, when training the GCN-DRL model, the parameters of the Deep Q function are saved as the "training experience." Therefore, unlike conventional decision algorithms that need to start from scratch for each new damage scenario, the GCN-DRL model can use the "training experience" from previous training results as long as the new damaged pipes have been considered in the training model. Consequently, high computational efficiency is achieved, which is advantageous for emergency response.

To demonstrate the benefits of transfer learning, the performance of the GCN-DRL model and computational time based on transfer learning for new damage scenarios is compared with those by the conventional methods. The new damages are randomly chosen from a subset of the predicted pipe damages (i.e., Figure 8b) as the initial damage situation. Figure 14 shows the selected damage situations with 36, 31, and 24 damaged pipes. The "

TABLE 4 Summary of SRI of WDN recovery based on repair sequence by different methods as well as the corresponding computational time for different damage scenarios

Scenario no./method	Performance indicator	S1	S2	S3	S4	S5
1 (36 damaged pipes)	SRI	35.449	34.286	35.197	33.743	13.712
	Time	6 min	3 min	15 min	4.0 h	~1 min
2 (31 damaged pipes)	SRI	33.243	31.746	32.414	29.674	20.406
	Time	5 min	4 min	11 min	2.6 h	~1 min
3 (24 damaged pipes)	SRI	27.551	27.517	27.548	26.165	22.742
	Time	4 min	4 min	10 min	2.1 h	~1 min

training experience" of the pre-trained model described in Section 4.2 is loaded to the GCN-DRL model (S1). Methods S2, S3, S3, and S5 are used for comparison purposes. The pre-trained GCN-DRL was trained with 10 episodes for each new WDN damage situation.

Table 4 summarizes the performance as well as the corresponding computational time to determine the repair sequence by different methods on the new damage scenarios. The require sequence identified by GCN-DRL model (S1) with transfer learning achieved the highest SRI value among all the methods, including the highest resilience. The SRI value of the repair sequence by S1 is larger than the other four repair methods by 1.16, 0.252, 1.706, and 21.737 under the earthquake scenarios causing 36 damaged pipes. The SRI value based on repair decision by S1 improved by 0.034, 0.003, 1.386, and 4.809 for the earthquake scenario causing 24 damaged pipes.

The results indicate that the larger the number of pipes damaged, the more advantages of GCN-DRL in achieving an optimal decision sequence than conventional methods. This makes sense since the larger the number of pipes damaged, the more difficult it takes to identify the global optimum with conventional methods. This is also an indication of the strength of the GCN-DRL model in making global optimal decisions among a large decision space.

In terms of the computational time for decisions, the use of transfer learning significantly reduced the time needed for the GCN-DRL model to determine the optimal repair sequence. The computational time is comparable to those needed by the greedy search algorithm and diameter-based prioritization method. It is noted that the GCN-DRL model significantly outperformed the GA method, another general-purpose metaheuristic global optimization method, both in terms of performance and computational efficiency.

5 | CONCLUSION

Optimal repair decisions play an important role in improving WDN resilience by accelerating the post-disasters recovery of the system performance. This study proposed a novel AI based decision-making model to achieve a resilience-oriented restoration plan. A resilience evaluation framework is first developed, which consists of a model for pipe failure prediction, a model for WDN performance measurement, and a model for WDN resilience quantification. The SRI is proposed for the system resilience quantification, which is defined based on the time evolution of PDW during the recovery process. The PDW considers the NSDs, which measure the extent of the post-hazards dynamic water demands at WDN supply nodes so that the demands are met, weighted by the relative importance of these nodes. With SRI, a novel GCN-DRL ML model is developed to determine the optimal repairing decision. The GCN-DRL model combines the advantages of DRL and GCN. The GCN is used to embed the WDN including the topological connections and information of NSDs at each node. The DRL framework is used to train the GCN to learn and determine the optimal repair actions under a given damage situation.

The GCN-DRL model is demonstrated to determine the optimal repair sequence of a testbed WDN subjected to earthquake damages. Three different damage scenarios are analyzed considering the magnitudes of the earthquake, distance to the epicenter, soil type, pipe deterioration, and so forth. The performance of the pipe repair sequences by the GCN-DRL model is compared with the results by four traditional decision-making methods. The results show that the GCN-DRL model consistently identified repairing sequences that lead to the highest SRI under different damage scenarios. Besides, the transfer learning strategy can be used to train the GCN-DRL model for new damage scenarios by taking the advantage of the prior training experience. The transfer learning strategy was demonstrated in three new damage situations of the WDN. The results show that the transfer learning of GCN-DRL decision-making model achieved the most resilient WDN recovery with significantly shortened computational time. Therefore, the new GCN-DRL model is promising to be a high-performance robust decision-support tool for post-hazard repairing decisions to ensure resilient WDN

recovery. However, it is noted that conventional methods such as S2 and S3 feature simplicity and good interpretability. The proposed GCN-DRL model is more advantageous with the increasing dimension of the decision space (associated with a larger number of damages). As with most ML models, improvement of interpretability is an area that requires further research.

It is noted that several simplified assumptions are used in this study, which is intended to allow the analyses to focus on the most important contributions, that is, the development of the innovative GCN-DRL-based framework to support WDS recovery decisions. For example, the repairing time for the damaged pipe is assumed to be only dependent upon the number of leakage points along the pipe. However, a more advanced model for pipe repairing time and repair crew task assignment can be easily accommodated. The study only considered the damages of pipes. Damages to the water towers or pump stations are not considered, although this is a common assumption used in most existing WSN research. The damage assessment and recovery analyses can readily incorporate other components of the WDS. Besides, this study used the water satisfaction degree to quantify the serviceability of the post-hazard performance of the water distribution system. Further advancement can incorporate multiple measurement metrics to quantify the WDN performance. Overall, the GCN-DRL model framework is developed with scalability and generality in mind, which can be readily adapted to analyze different types of WDS and accommodate more sophisticated assumptions.

REFERENCES

Ahmadlou, M., & Adeli, H. (2010). Enhanced probabilistic neural network with local decision circles: A robust classifier. *Integrated Computer-Aided Engineering*, *17*(3), 197–210.

Alam, K. M. R., Siddique, N., & Adeli, H. (2020). A dynamic ensemble learning algorithm for neural networks. *Neural Computing and Applications*, *32*(12), 8675–8690.

Alliance, A. (2001). *Seismic fragility formulations for water systems, Part I-Guideline*.

Almoghathawi, Y., Barker, K., & Albert, L. A. (2019). Resilience-driven restoration model for interdependent infrastructure networks. *Reliability Engineering & System Safety*, *185*, 12—23.

Andriotis, C., & Papakonstantinou, K. (2019). Managing engineering systems with large state and action spaces through deep reinforcement learning. *Reliability Engineering & System Safety*, *191*, 106483.

Balut, A., Brodziak, R., Bylka, J., & Zakrzewski, P. (2018). Battle of post-disaster response and restauration (BPDRR). *Proceedings of the 1st International Water Distribution System Analysis/Computing and Control in the Water Industry Joint Conference*, Kingston, Ontario, Canada (pp. 23–25).

Bellman, R. (1952). On the theory of dynamic programming. *Proceedings of the National Academy of Sciences of the United States of America*, *38*(8), 716.

Brink, S. A., Davidson, R. A., & Tabucchi, T. H. (2012). Strategies to reduce durations of post-earthquake water service interruptions in Los Angeles. *Structure and Infrastructure Engineering*, *8*(2), 199–210.

Castro-Gama, M., & Quintiliani, C. (2018). After earthquake post-disaster response using a many-objective approach, a greedy and engineering interventions. *WDSA/CCWI Joint Conference Proceedings,* Kingston, Ontario, Canada.

Chen, S., Dong, J., Ha, P., Li, Y., & Labi, S. (2021). Graph neural network and reinforcement learning for multi-agent cooperative control of connected autonomous vehicles. *Computer-Aided Civil and Infrastructure Engineering*, *36*(7), 838–857.

Cimellaro, G. P., Tinebra, A., Renschler, C., & Fragiadakis, M. (2016). New resilience index for urban water distribution networks. *Journal of Structural Engineering*, *142*(8), C4015014.

Cormen, T. H., Leiserson, C. E., Rivest, R. L., & Stein, C. (2009). *Introduction to algorithms.* MIT Press.

Diao, K., Sweetapple, C., Farmani, R., Fu, G., Ward, S., & Butler, D. (2016). Global resilience analysis of water distribution systems. *Water Research*, *106*, 383–393.

Didier, M., Baumberger, S., Tobler, R., Esposito, S., Ghosh, S., & Stojadinovic, B. (2018). Seismic resilience of water distribution and cellular communication systems after the 2015 Gorkha Earthquake, *Journal of Structural Engineering*, *144*(6), 04018043.

Eidinger, J., & Tang, A. (2014). *Christchurch, New Zealand Earthquake sequence of M 7.1 September 04, 2010 M 9.3 February 22, 2011 M6. 0 June 13, 2011: Lifeline performance*. American Society of Civil Engineers.

Federal Emergency Management Agency. (2003). *Multi-hazard loss estimation methodology: Earthquake model.* Department of Homeland Security, FEMA.

Fragiadakis, M., & Christodoulou, S. E. (2014). Seismic reliability assessment of urban water networks. *Earthquake Engineering & Structural Dynamics*, *43*(3), 357–374.

González, A. D., Dueñas-Osorio, L., Sánchez-Silva, M., & Medaglia, A. L. (2016). The interdependent network design problem for optimal infrastructure system restoration. *Computer-Aided Civil and Infrastructure Engineering*, *31*(5), 334–350.

Guo, J., Wang, Q., & Li, Y. (2021). Semi-supervised learning based on convolutional neural network and uncertainty filter for façade defects classification. *Computer-Aided Civil and Infrastructure Engineering*, *36*(3), 302–317.

Guo, J., Wang, Q., Li, Y., & Liu, P. (2020). Façade defects classification from imbalanced dataset using meta learning-based convolutional neural network. *Computer-Aided Civil and Infrastructure Engineering*, *35*(12), 1403–1418.

Hernadez, E., Hoagland, S., & Ormsbee, L. (2016). Water distribution database for research applications. *World Environmental and Water Resources Congress 2016*, West Palm Beach, FL (pp. 465–474).

Hossain, N. U. I., Nur, F., Hosseini, S., Jaradat, R., Marufuzzaman, M., & Puryear, S. M. (2019). A Bayesian network based approach for modeling and assessing resilience: A case study of a full service deep water port, *Reliability Engineering & System Safety*, *189*, 378–396.

Hosseini, S., Barker, K., & Ramirez-Marquez, J. E. (2016). A review of definitions and measures of system resilience. *Reliability Engineering & System Safety*, *145*, 47–61.

Hu, L., Liu, Z., Hu, W., Wang, Y., Tan, J., & Wu, F. (2020). Petri-net-based dynamic scheduling of flexible manufacturing system via

deep reinforcement learning with graph convolutional network. *Journal of Manufacturing Systems*, *55*, 1–14.

Jayaram, N., & Srinivasan, K. (2008). Performance-based optimal design and rehabilitation of water distribution networks using life cycle costing. *Water Resources Research*, *44*(1), W01417.

Jeong, J. H., Jo, H., & Ditzler, G. (2020). Convolutional neural networks for pavement roughness assessment using calibration-free vehicle dynamics. *Computer-Aided Civil and Infrastructure Engineering*, *35*(11), 1209–1229.

Karakoc, D. B., Almoghathawi, Y., Barker, K., González, A. D., & Mohebbi, S. (2019). Community resilience-driven restoration model for interdependent infrastructure networks. *International Journal of Disaster Risk Reduction*, *38*, 101228.

Kipf, T. N., & Welling, M. (2016). Semi-supervised classification with graph convolutional networks. *arXiv preprint arXiv:1609.02907*.

Klise, K., Hart, D., Bynum, M., Hogge, J., Haxton, T., Murray, R., & Burkhardt, J. (2020). Water network tool for resilience (WNTR) user manual. Sandia National Lab.(SNL-NM).

Lambert, A. (2001). What do we know about pressure-leakage relationships in distribution systems. *IWA Conference and Systems Approach to Leakage Control and Water Distribution System Management*, Brno, Czech Republic.

LeCun, Y., Bottou, L., Bengio, Y., & Haffner, P. (1998). Gradient-based learning applied to document recognition. *Proceedings of the IEEE*, *86*(11), 2278–2324.

Li, Y., Yu, R., Shahabi, C., & Liu, Y. (2017). Diffusion convolutional recurrent neural network: data-driven traffic forecasting. *arXiv preprint arXiv:1707.01926*.

Liu, W., & Song, Z. (2020). Review of studies on the resilience of urban critical infrastructure networks. *Reliability Engineering & System Safety*, *193*, 106617.

Liu, W., Song, Z., Ouyang, M., & Li, J. (2020). Recovery-based seismic resilience enhancement strategies of water distribution networks. *Reliability Engineering & System Safety*, *203*, 107088.

Liu, Y., Peng, Y., Wang, B., Yao, S., & Liu, Z. (2017). Review on cyber-physical systems, *IEEE/CAA Journal of Automatica Sinica*, *4*(1), 27–40.

Mazumder, R. K., Fan, X., Salman, A. M., Li, Y., & Yu, X. (2020). Framework for seismic damage and renewal cost analysis of buried water pipelines. *Journal of Pipeline Systems Engineering and Practice*, *11*(4), 04020038.

Mnih, V., Kavukcuoglu, K., Silver, D., Graves, A., Antonoglou, I., Wierstra, D., & Riedmiller, M. (2013). Playing Atari with deep reinforcement learning. *arXiv preprint arXiv:1312.5602*.

Mnih, V., Kavukcuoglu, K., Silver, D., Rusu, A. A., Veness, J., Bellemare, M. G., Graves, A., Riedmiller, M., Fidjeland, A. K., & Ostrovski, G. (2015). Human-level control through deep reinforcement learning. *Nature*, *518*(7540), 529–533.

Moscato, P. (1989). *On genetic crossover operators for relative order preservation*. Caltech Concurrent Computation Program, Report C3P-778.

Nair, G. S., Dash, S. R., & Mondal, G. (2018). Review of pipeline performance during earthquakes since 1906. *Journal of Performance of Constructed Facilities*, *32*(6), 04018083.

Nurre, S. G., Cavdaroglu, B., Mitchell, J. E., Sharkey, T. C., & Wallace, W. A. (2012). Restoring infrastructure systems: An integrated network design and scheduling (INDS) problem, *European Journal of Operational Research*, *223*(3), 794–806.

O'Rourke, M., & Ayala, G. (1993). Pipeline damage due to wave propagation. *Journal of Geotechnical Engineering*, *119*(9), 1490–1498.

O'Rourke, T. D., Jeon, S. -S., Toprak, S., Cubrinovski, M., Hughes, M., van Ballegooy, S., & Bouziou, D. (2014). Earthquake response of underground pipeline networks in Christchurch, NZ. *Earthquake Spectra*, *30*(1), 183–204.

Ouyang, M., & Wang, Z. (2015). Resilience assessment of interdependent infrastructure systems: With a focus on joint restoration modeling and analysis. *Reliability Engineering & System Safety*, *141*, 74–82.

Paez, D., Filion, Y., Castro-Gama, M., Quintiliani, C., Santopietro, S., Sweetapple, C., Meng, F., Farmani, R., Fu, G., & Butler, D. (2020). Battle of postdisaster response and restoration. *Journal of Water Resources Planning and Management*, *146*(8), 04020067.

Paez, D., Fillion, Y., & Hulley, M. (2018). Battle of post-disaster response and restauration (BPDRR): Problem description and rules. *1st International Water Distribution System Analysis /Computing and Control in the Water Industry Joint Conference*, Kingston, Ontario, Canada.

Paszke, A., Gross, S., Massa, F., Lerer, A., Bradbury, J., Chanan, G., Killeen, T., Lin, Z., Gimelshein, N., & Antiga, L. (2019). Pytorch: An imperative style, high-performance deep learning library. *Advances in Neural Information Processing Systems*, Vancouver, Canada (pp. 8026–8037).

Pereira, D. R., Piteri, M. A., Souza, A. N., Papa, J. P., & Adeli, H. (2020). Fema: A finite element machine for fast learning. *Neural Computing and Applications*, *32*(10), 6393–6404.

Pinzinger, R., Deuerlein, J., Wolters, A., & Simpson, A. (2011). Alternative approaches for solving the sensor placement problem in large networks. In E. R. Beighley, & M. W. Killgore (Eds.), *World Environmental and Water Resources Congress 2011: Bearing Knowledge for Sustainability* (pp. 314–323). American Society of Civil Engineers.

Prasad, T. D., & Park, N. -S. (2004). Multiobjective genetic algorithms for design of water distribution networks. *Journal of Water Resources Planning and Management*, *130*(1), 73–82.

Pudasaini, B., & Shahandashti, M. (2020). Topological surrogates for computationally efficient seismic robustness optimization of water pipe networks. *Computer-Aided Civil and Infrastructure Engineering*, *35*(10), 1101–1114.

Pudasaini, B., & Shahandashti, S. (2018). Identification of critical pipes for proactive resource-constrained seismic rehabilitation of water pipe networks. *Journal of Infrastructure Systems*, *24*(4), 04018024.

Rafiei, M. H., & Adeli, H. (2017). A new neural dynamic classification algorithm. *IEEE Transactions on Neural Networks and Learning Systems*, *28*(12), 3074–3083.

Romero, N., O'Rourke, T., Nozick, L., & Davis, C. (2010). Seismic hazards and water supply performance. *Journal of Earthquake Engineering*, *14*(7), 1022–1043.

Rossman, L., Woo, H., Tryby, M., Shang, F., Janke, R., & Haxton, T. (2020). *Epanet 2.2 user manual*. EPA/600/R-20/133, U.S. Environmental Protection Agency.

Schafer, R. W. (2011). What is a Savitzky-Golay filter? [Lecture notes]. *IEEE Signal Processing Magazine*, *28*(4), 111–117.

Shahata, K., & Zayed, T. (2016). Integrated risk-assessment framework for municipal infrastructure. *Journal of Construction Engineering and Management*, *142*(1), 04015052.

Sharkey, T. C., Nurre Pinkley, S. G., Eisenberg, D. A., & Alderson, D. L. (2021). In search of network resilience: An optimization-based view, *Networks*, *77*(2), 225–254.

Shi, P., & O'Rourke, T. D. (2008). *Seismic response modeling of water supply systems*. Multidisciplinary Center for Earthquake Engineering Research.

Tang, K., Cao, Y., Chen, C., Yao, J., Tan, C., & Sun, J. (2021). Dynamic origin-destination flow estimation using automatic vehicle identification data: A 3D convolutional neural network approach. *Computer-Aided Civil and Infrastructure Engineering*, *36*(1), 30–46.

Todini, E. (2000). Looped water distribution networks design using a resilience index based heuristic approach. *Urban Water*, *2*(2), 115–122.

Uber, J., Janke, R., Murray, R., & Meyer, P. (2004). Greedy heuristic methods for locating water quality sensors in distribution systems. *Critical Transitions in Water and Environmental Resources Management*, Salt Lake City, UT (pp. 1–9).

Wagner, J. M., Shamir, U., & Marks, D. H. (1988). Water distribution reliability: simulation methods. *Journal of Water Resources Planning and Management*, *114*(3), 276–294.

Wang, F., Song, G., & Mo, Y. L. (2021). Shear loading detection of through bolts in bridge structures using a percussion-based one-dimensional memory-augmented convolutional neural network. *Computer-Aided Civil and Infrastructure Engineering*, *36*(3), 289–301.

Wang, M., Yu, L., Zheng, D., Gan, Q., Gai, Y., Ye, Z., Li, M., Zhou, J., Huang, Q., & Ma, C. (2019). Deep graph library: Towards efficient and scalable deep learning on graphs. *arXiv preprint arXiv:1909.01315*.

Q13 Wang, Y., Hou, S., & Wang, X. (2020). Reinforcement learning-based bird-view automated vehicle control to avoid crossing traffic. *Computer-Aided Civil and Infrastructure Engineering*, *36*(7), 890–901.

Wiering, M., & Van Otterlo, M. (2012). *Reinforcement learning* (Adaptation, Learning, and Optimization Series, Vol. 12(3). Springer.

Q14 Yan, Z., Ge, J., Wu, Y., Li, L., & Li, T. (2020). Automatic virtual network embedding: A deep reinforcement learning approach with graph convolutional networks. *IEEE Journal on Selected Areas in Communications*, *38*(6), 1040–1057.

Yao, L., Dong, Q., Jiang, J., & Ni, F. (2020). Deep reinforcement learning for long-term pavement maintenance planning. *Computer-Aided Civil and Infrastructure Engineering*, *35*(11), 1230–1245.

Yu, Y., & Jin, C. (2008). Empirical peak ground velocity attenuation relations based on digital broadband records. *The 14th World Conference on Earthquake Engineering*, Beijing, China (pp. 13–17).

Zarghami, S. A., Gunawan, I., & Schultmann, F. (2018). Vulnerability analysis of water distribution networks using betweenness centrality and information entropy. *The 2nd IEOM European Conference on Industrial Engineering and Operations Management*, Paris, France.

Zhang, W., & Wang, N. (2016). Resilience-based risk mitigation for road networks. *Structural Safety*, *62*, 57–65.

Zhang, W., Wang, N., & Nicholson, C. (2017). Resilience-based post-disaster recovery strategies for road-bridge networks. *Structure and Infrastructure Engineering*, *13*(11), 1404–1413.

Zhao, D., Qin, H., Song, B., Han, B., Du, X., & Guizani, M. (2020). A graph convolutional network-based deep reinforcement learning approach for resource allocation in a cognitive radio network, *Sensors*, *20*(18), 5216.

Zhou, X., Tang, Z., Xu, W., Meng, F., Chu, X., Xin, K., & Fu, G. (2019). Deep learning identifies accurate burst locations in water distribution networks. *Water Research*, *166*, 115058.

How to cite this article: Fan, X., Zhang, X., & Yu X. (B). (2022). A graph convolution network-deep reinforcement learning model for resilient water distribution network repair decisions. *Comput Aided Civ Inf*, 1–19.
https://doi.org/10.1111/mice.12813